Published in final edited form as:
J Cereb Blood Flow Metab. 2008 September ; 28(9): 1564–1573. doi:10.1038/jcbfm.2008.44.

Necrostatin-1 Reduces Histopathology and Improves Functional Outcome After Controlled Cortical Impact In Mice

Zerong You, Ph.D.[1,2], **Sean I. Savitz, M.D.**[1,4], **Jinsheng Yang, Ph.D.**[1,2], **Alexei Degterev, Ph.D.**[5], **Junying Yuan, Ph.D.**[5], **Gregory D. Cuny, Ph.D.**[6], **Michael A. Moskowitz, M.D.**[1,3], and **Michael J. Whalen, M.D.**[1,2]

[1]Neuroscience Center and Massachusetts General Hospital, Harvard Medical School, Charlestown, MA 02129

[2]Department of Pediatrics, Massachusetts General Hospital, Harvard Medical School, Charlestown, MA 02129

[3]Department of Radiology, Massachusetts General Hospital, Harvard Medical School, Charlestown, MA 02129

[4]Department of Neurology, Beth Israel Deaconess Medical Center, Boston, MA

[5]Department of Cell Biology, Harvard Medical School, Boston, MA 02115

[6]Laboratory for Drug Discovery in Neurodegeneration, Brigham & Women's Hospital, Harvard Medical School, Cambridge, MA 02139

Abstract

Necroptosis is a newly identified type of programmed necrosis initiated by activation of tumor necrosis factor alpha (TNF) and Fas. Necrostatin-1 is a specific inhibitor of necroptosis that reduces ischemic tissue damage in experimental stroke models. We previously reported decreased tissue damage and improved functional outcome after controlled cortical impact (CCI) in mice deficient in TNF and Fas. Hence, we hypothesized that necrostatin-1 would reduce histopathology and improve functional outcome after CCI in mice. Compared to vehicle- or inactive analogue-treated controls, mice administered necrostatin-1 intracerebroventricularly prior to CCI had decreased cells with plasmalemma permeability in injured cortex and dentate gyrus at 6 h ($p < 0.05$), decreased brain tissue damage at 2 and 5 weeks after CCI ($p < 0.05$), improved motor performance (d 1–7, $p < 0.05$) and improved performance in a Morris water maze paradigm (d 8–14, $p < 0.01$) after CCI. Improved spatial memory was observed even when drug was administered 15 min after CCI ($p < 0.05$ for probe trials). Necrostatin-1 treatment did not reduce caspase-3-positive cells in dentate gyrus or cortex, consistent with a known caspase-independent mechanism of necrostatin-1. However, necrostatin-1 reduced brain neutrophil influx and microglial activation at 48 h ($p < 0.05$), suggesting a novel anti-inflammatory effect in traumatic brain injury (TBI). The data suggest that necroptosis plays a significant role in the pathogenesis of cell death and functional outcome after TBI, and that necrostatin-1 may have therapeutic potential for patients with TBI and perhaps other forms of acute brain injury.

Address correspondence to: Michael Whalen, M.D., Department of Pediatric Critical Care Medicine, Massachusetts General Hospital and Harvard Medical School, 149 13th Street, Charlestown, MA 02129. Phone: 617-724-4380; Fax: 617-724-4391; MWhalen@Partners.org.

Introduction

Necroptosis is a recently discovered, regulated form of programmed necrosis initiated by activation of tumor necrosis factor alpha (TNF) and/or Fas that is distinct from caspase-dependent apoptotic cell death (Degterev et al., 2005). In susceptible cell types such as Jurkat cells and U937 monocytes, TNF or Fas induced cell death occurs by caspase-mediated apoptosis. However, in the presence of caspase inhibitors, these cell types die in response to TNF or Fas activation with ultrastructural features of necrosis (Denecker et al. 2001a; Denecker et al. 2001b; Holler et al. 2000; Matsumura et al. 2000; Vanden Berghe et al. 2004a; Vanden Berghe et al. 2002; Vanden Berghe et al. 2004b; Vercammen et al. 1998a; Vercammen et al. 1998b; Vercammen et al. 1997). This alternative, death receptor-mediated, necrosis-like mode of cell death has been termed necroptosis (Degterev et al. 2005).

Using an in vitro cell death assay of U937 cells exposed to TNF and ZVAD to induce necroptosis, a library screen of chemical compounds yielded a novel class of small molecule necroptosis inhibitors known as necrostatins (Degterev et al. 2005). Necrostatin-1 is a specific and potent inhibitor of necroptosis; it does not protect against caspase-dependent apoptosis, or against nonspecific oxidative stress-induced necrosis (Degterev et al. 2005). Recently, necrostatin-1 was shown to dose-dependently reduce infarction size with a wide therapeutic window in a mouse middle cerebral artery occlusion (MCAO) stroke model, suggesting that necroptosis may be an important mode of ischemic cell death in vivo (Degterev et al. 2005).

Here, we tested the hypothesis that necroptosis contributes to cell death after TBI, and that treatment with necrostatin-1 would reduce histopathology and functional deficits after controlled cortical impact (CCI) in mice. We found that necrostatin-1 reduced acute cellular plasmalemma permeability, short- and long-term tissue damage, and motor and cognitive deficits in mice subjected to CCI. The data suggest an important role for necroptosis in the pathogenesis of TBI, and suggest that necrostatin-1 may be a novel therapeutic agent for the treatment of patients with head injury and perhaps other acute central nervous system disorders that feature necroptosis as a mode of cell death.

Materials and Methods

For all studies, investigators were masked to treatment during surgery, data acquisition, and analysis.

Controlled cortical impact

The controlled cortical impact (CCI) model was used as previously described with minor modifications (Bermpohl et al. 2007). The trauma protocol was approved by the Massachusetts General Hospital Institutional Animal Care and Use Committee and complied with the NIH Guide for the Care and Use of Laboratory Animals. Mice (6–12 weeks of age) were anesthetized with 4% isoflurane (Anaquest, Memphis, TN) in 70% N_2O and 30% O_2 using a Fluotec 3 vaporizer (Colonial Medical, Amherst, NH) and positioned in a stereotaxic frame. Anesthesia was maintained using 2–3% isoflurane. A 5 mm craniotomy was made using a portable drill and trephine over the left parieto-temporal cortex, and the bone flap was removed. Mice were then subjected to CCI using a pneumatic cylinder with a 3-mm flat-tip impounder, velocity 6 m/s, set depth of 0.6 (for immunohistochemical studies requiring preserved cortical tissue) or 1.0 mm (for histopathological and behavioral studies), and 100 ms impact duration. The scalp was sutured closed and mice returned to their cages to recover from anesthesia.

Administration of necrostatins and related compounds

Necrostatin-1 (5-[(7-chloro-1H-indol-3-yl)methyl]-3-methyl-2,4-imidazolidinedi-one) (Teng et al. 2005), vehicle, or an inactive analogue of necrostatin-1 (5-[(7-chloro-1H-indol-3-yl) methyl]-1,3-dimethyl-2,4-imidazolidinedione (6 ul each) was administered into the left cerebral ventricle (co-ordinates relative to bregma: 0.1mm posterior, 1 mm lateral, 2 mm deep) before or at various times after CCI. For all experiments, a 4 mM solution of necrostatin-1 in methyl-beta-cyclodextrin (Sigma, St. Louis, MO) was used.

Assessment of lesion Volume

Morphometric image analysis (MCID, Imaging Research Inc, St. Catherines, Ontario, Canada) was used to determine lesion volume and brain tissue loss after CCI. Mice were deeply anesthetized with isoflurane, decapitated, and brains were removed and frozen in nitrogen vapor. Coronal brain sections (12 μm) were cut on a cryostat at 0.5 mm intervals from anterior to the posterior and mounted on poly-L-lysine-coated slides. Sections were stained with hematoxylin and the area of the lesion was quantitated using image analysis (Bermpohl et al. 2007). Lesion volume was expressed in mm^3.

Evaluation of motor and Morris water maze performance

Vestibulomotor function was assessed using a wire-grip test (Hall 1989). Mice were placed on a metal wire (45 cm long) suspended 45 cm above a foam pad and were allowed to traverse the wire for 60 s. The latency that a mouse remained on the wire within a 60 s interval was measured, and wire grip scores were quantitated using a 5-point scale (Bermpohl et al. 2006). A score of one point was given if the mouse failed to hold on to the wire with both sets of fore paws and hind paws together; two points were given if the mice held on to the wire with both forepaws and hind paws but not the tail; three points were given if the mouse used its tail along with both forepaws and both hindpaws; four points were given if the mouse moved along the wire on all four paws plus tail; and five points were given if mice that scored four points also ambulated down one of the posts used to support the wire. Mice that were unable to remain on the wire for less than 30 s were given a score of zero. The wire grip test was performed in triplicate and an average value calculated for each mouse on each day of testing.

The Morris water maze (MWM) task was used to evaluate spatial memory performance as previously described with minor modifications (Bermpohl et al. 2007). The apparatus consisted of a white pool (83 cm diameter, 60 cm deep) filled with water to 29 cm depth with several highly visible cues located on the walls of each of the four quadrants. Water temperature was maintained 21–25°C. A clear plexiglass goal platform 10 cm in diameter was positioned 0.5 cm below the water's surface approximately 15 cm from the southwest wall. Each mouse was subjected to 1 or 2 trials per day. For each trial, mice were randomized to one of four starting locations (north, south, east, or west) and placed in the pool facing the wall. Mice were given a maximum of 60 s to find the submerged platform. If the mouse failed to reach the platform by 60 s, it was placed on the platform by the experimenter and allowed to remain there for 10 seconds. Mice were placed in a warming chamber for at least 4 minutes between trials. The average latency to the goal platform from the four starting locations was recorded as the latency for that trial. To control for possible differences in visual acuity or sensorimotor function between groups, two subsequent trials were performed using a visible platform raised 0.5 cm above the surface of the water. Following the visible platform trials, a probe trial was performed on the following day in which the mouse was given 60 s to swim in the tank with the goal platform removed. The time spent in the target quadrant (probe time) was recorded for each mouse. Performance in the MWM was quantitated by latency to the platform.

Administration of propidium iodide and detection of PI-positive cells

Propidium iodide (PI; 10mg/ml, Sigma, St. Louis, MO) was diluted in 0.9% NaCl and 1 mg/kg was administered 1 h prior to sacrifice by intraperitoneal injection in a total volume of not more than 100 ul. Mice were killed at 6 h after CCI, the brains frozen in nitrogen vapor, and cryostat brain sections (12 um) were cut at 150–200 um intervals from anterior to posterior hippocampus. Cryostat sections were placed on poly-L-lysine slides and stored at −80°C. For detection of PI-labeled cells, brain sections were fixed in 100% ethanol for 10 min at room temperature, coverslipped with Permount (Biomeda, Foster City, CA) and photographed on a Nikon Eclipse T300 fluorescence microscope (Tokyo, Japan) using excitation/emission filters 568/585 for PI.

Caspase-3, neutrophil and astrocyte immunohistochemistry

At 48 h after CCI, mice were anaesthetized with isoflurane and the brain rapidly removed intact and frozen at −80°C. Coronal brain sections (12 μm) were placed on poly-L-lysine coated slides and were fixed in 100% ethanol at room temperature for 10 min. Slides were washed in phosphate buffered saline (pH 7.4; PBS). Sections were blocked for 30 min in PBS with 3% normal goat serum and then incubated over night at 4°C with rabbit polyclonal anti-caspase-3 antibody (1:1000, CM1, Idun Pharmaceuticals, La Jolla, CA). The CM-1 antibody reacts specifically with the p18 fragment of cleaved caspase-3 but not with full-length caspase-3 (Srinivasan et al. 1998). Sections were then washed in PBS and incubated with goat anti-rabbit IgG-Cy-3 conjugate (1:300, Jackson ImmunoResearch, West Grove, PA) for 60 min. To detect neutrophils and astrocytes, frozen brain sections were air-dried and fixed in 100% ethanol at room temperature for 10 min. Slides were washed in PBS (pH 7.4) and blocked for 30 min in PBS with 3% normal goat serum, then incubated overnight at 4°C with PE-conjugated rat anti-mouse neutrophil antibody M1/70 (1:200; BD-Biosciences, Franklin Lakes, NJ) or with Cy3-conjugated monoclonal anti-glial fibrillary acidic protein (GFAP) antibody (1:2,000; Sigma, St. Louis, MO). Sections were washed in PBS, rinsed with water, air-dried and cover-slipped with Crystal mount (Biomeda, Foster city, CA). Sections were analyzed on a Nikon Eclipse T300 fluorescence microscope. Excitation/emission filters were 568/585 for both M1/70-PE and Cy3.

Assessment of PI-positive, neutrophil and caspase-3-positive cell counts

Cell counts were determined as previously described (Bermpohl et al. 2007). The regions of interest in injured cortex (200× microscopic fields, 1100 × 1100 um) for PI-and caspase-3-positive cell counts were a cortical field at the medial edge and a cortical field at the lateral edge of the contusion. Three coronal brain sections separated by at least 150 um were randomly sampled from brain regions between bregma −1.90 to −2.70 for a total of six × 200 cortical fields assessed per animal. For cell counts in dentate gyrus, two adjacent × 200 fields (1100 × 1100 um) encompassing the upper and lower blades of the dentate gyrus were evaluated in the three brain sections selected for cortical cell counts (above). Cell count data for each mouse were reported as the average of the cortical or hippocampal fields.

For the estimation of neutrophils in injured cortex, cortical brain fields (× 200; 1100 ×1100 um) from three brain sections separated by at least 150 mm and within the approximate center of the contusion were selected for analysis. Neutrophils were photographed and quantitated in three × 200 cortical fields randomly chosen from each brain section. Thus, a total of nine × 200 fields were analyzed per mouse. From these data, an average neutrophil count per × 200 field was obtained for each animal.

Microglia immunohistochemistry

At 48 h after CCI mice were anesthetized with isoflurane and transcardially perfused with 4% paraformaldehyde. The brain was removed and frozen in nitrogen vapor, and stored at −80°C. Coronal brain sections (12 μm) were placed on poly-L-lysine-coated slides and stored at −80° C. Brain sections were washed with PBS, rinsed with water, air-dried and cover-slipped with crystal/mount (Biomeda, Foster city, CA, USA), and analyzed on a Nikon Eclipse T300 fluorescence microscope. Excitation/emission filters were 568/585 for both M1/70-PE and Cy-3.

Microglia staining was performed using paraformaldehyde-fixed brain tissue. Cryostat-fixed brain sections were treated with 1% hydrogen peroxide in PBS. The slides were blocked in PBS with 3% normal goat serum for 1 h and incubated overnight at 4°C with rabbit anti-Iba-1 antibody (1:200; Wako Pure Chemical Industries Ltd., Osaka, Japan). The sections were then washed in PBS with 1% normal goat serum and incubated with biotinylated goat anti-rabbit immunoglobulin G (1:200; Vector Laboratories, Burlingame, CA, USA) antibody for 1 h. After washing, the signal was detected using an ABC kit (Vector Labs) and diaminobenzidine (Vector Labs).

Quantitation of astrocytes and activated microglia in mouse cortex after CCI

For the analysis of GFAP-positive astrocytes or Iba-1-positive microglia, photomicrographs of × 200 fields from the medial and lateral edges of the contusion were analyzed from three brain sections as described above (cell counts). Using MCID image analysis software, activated GFAP-positive astrocytes or IBA-1-positive microglia were quantified as previously described (Bermpohl et al. 2007).

Statistical analyses

Data are mean ± SEM. Cell count data were analyzed by rank sum test. Lesion volume and brain tissue loss data, and probe trial data were analysed by ANOVA on ranks and rank sum tests. Motor and Morris water maze test data (hidden and visible platform acquisition latencies) were analyzed by two factor repeated measures ANOVA (group × time). For all comparisons, $p < 0.05$ was regarded as significant.

Results

All animals survived CCI and the experimental period. No overt toxic effects of necrostatin-1, inactive analogue, or vehicle treatment were observed in any of the mice studied.

Necrostatin-1 inhibits brain tissue damage after CCI

We first examined the effect of necrostatin-1 treatment on brain lesion size after CCI. In animals administered necrostatin-1 immediately prior to CCI (pretreated), lesion size was significantly reduced by approximately 30–40% compared to pretreatment with vehicle or inactive analogue (Figure 1A). Pretreatment with necrostatin-1 also reduced lesion size assessed at 35 days after CCI (Figure 1A), suggesting that protection against brain tissue damage is a persistent effect of necrostatin-1 in our CCI model. To determine the therapeutic window for necrostatin-1, drug or vehicle was administered to mice before or at various times after CCI and lesion size assessed at two weeks. Figure 1B shows that administration of necrostatin-1 pre-injury or at 15 but not 30 min after CCI significantly reduced brain lesion size.

Necrostatin-1 improves recovery of motor performance after CCI

We next determined the effect of necrostatin-1 treatment on postinjury motor function. No difference in baseline motor function before CCI was observed between groups of mice

administered drug, vehicle, or inactive analogue (Figure 2). Following CCI, recovery of motor function was significantly improved in necrostatin-1-treated mice versus mice treated with inactive analogue or vehicle (Figure 2A, $p < 0.05$ for group effects). In contrast, mice administered necrostatin-1 at 5 min postinjury had wire grip performance similar to vehicle-treated mice, suggesting a short therapeutic window for necrostatin-1 with respect to motor dysfunction (Figure 2B).

Necrosatin-1 improves spatial memory acquisition after CCI

To examine the effect of necrostatin-1 on postinjury cognitive function, we assessed performance of injured mice pretreated with necrostatin-1, inactive analogue, or vehicle in a Morris water maze paradigm. Mice administered necrostatin-1 prior to CCI had significantly improved latency to the hidden platform compared to vehicle- or inactive analogue-treated mice, whereas all three groups had similar performance in visible platform tests (Figure 3A). The protective effect of necrostatin-1 in injured mice could not be attributed to effects on baseline MWM performance as naïve (uninjured) mice administered necrostatin-1 or vehicle did not differ in acquisition of hidden or visible platform tests (Figure 3B). Results of probe trial testing are shown in Figure 3C. Injured mice pretreated with necrostatin-1 performed similarly to sham-injured mice (administered vehicle or necrostatin-1) and significantly better compared to injured vehicle- or inactive analogue-treated mice. No difference in probe trials was observed between sham-injured vehicle- or drug-treated mice. In a separate set of experiments, mice were treated with necrostatin-1 or vehicle at various times after CCI and MWM performance was assessed as above. Although no significant differences between groups were observed in hidden platform trials with limited numbers of mice per group (data not shown), mice given necrostatin-1 at 5 or 15 minutes postinjury had significantly improved probe trial performance vs. vehicle treated animals ($p < 0.05$, Figure 3C).

Necrostatin-1 reduces acute plasmalemma permeability in injured cells after CCI

Plasmalemma permeability is a hallmark of necrotic, including necroptotic, cell death. To begin to address cellular mechanisms of reduced postinjury tissue damage, we assessed the effect of necrostatin-1 treatment on loss of plasmalemma integrity in cortical and hippocampal brain regions using in vivo propidium iodide labeling. Compared to vehicle treated mice, mice administered necrostatin-1 prior to CCI had decreased numbers of PI-positive cortical cells at 6 h after CCI in injured cortex and dentate gyrus brain regions ($p < 0.05$, Figure 4A, B), suggesting reduction of necrosis-like cellular injury. Because plasmalemma permeability may also be associated with late apoptotic mechanisms, we next assessed the effect of necrostatin-1 on caspase-3 activation in the same brain regions used to assess plasmalemma integrity, at 48 h after CCI. Figure 5A shows representative immunohistochemical detection of activated caspase-3 in injured cortex and dentate gyrus. No difference in numbers of cells with activated caspase-3 were observed between necrostatin-1 and vehicle-treated mice (Figure 5B).

Necrostatin-1 inhibits cellular neuroinflammation after CCI

To assess the potential effect of necrostatin-1 on neuroinflammation after CCI, we examined brain neutrophil counts, astrocytosis, and the microglial response to CCI in injured mouse cortex at 48 h in mice pretreated with necrostatin-1 or vehicle. This time point was chosen because all three of these inflammatory markers are robust in injured brain at 48 h (Bermpohl et al. 2007). Figure 6A shows that brain neutrophil counts in injured cortical brain regions were decreased by approximately 50% in necrostatin-1-treated mice. Similarly, necrostatin-1 markedly inhibited the staining intensity of activated microglia detectable with Iba-1 antibody (Figure 6B). In contrast, immunohistochemical density analysis of astrocytes showed no differences between groups (data not shown).

Discussion

We provide strong evidence that necroptosis is an important mechanism of cell death and neurological dysfunction after TBI. Necrostatin-1, a specific inhibitor of necroptosis (Degterev et al. 2005), reduced acute cellular injury, brain tissue damage, motor dysfunction, and spatial learning deficits after CCI in mice. Indeed, necrostatin treatment recapitulated all of the protective effects of TNF/Fas knockout in our CCI model, consistent with the known mechanism of action of necrostatins in cultured cells (Degterev et al. 2005). Importantly, clinically relevant effects of necrostatin-1 on learning and memory deficits were observed even when necrostatin-1 was administered 15 minutes after CCI. Necrostatin-1 treatment also markedly suppressed the neutrophil and microglial responses to CCI, suggesting a heretofore-unreported anti-inflammatory effect in acute brain injury. The data suggest a fundamental role for necroptosis in the pathogenesis of TBI.

Two lines of evidence suggest that necrostatin-1 specifically inhibits necroptosis in our CCI model. First, pretreatment with necrostatin-1 reduced the numbers of cells with loss of plasmalemma integrity, a hallmark of necroptosis, in cortex and dentate gyrus 6 h after CCI. Second, necrostatin-1 did not reduce the number of caspase-3 positive cells in cortex or dentate gyrus at 48 h after CCI, a time of maximal cleaved caspase-3 expression in our CCI model. These findings are consistent with in vitro data showing a specific effect of necrostatin-1 on programmed necrosis (Degterev et al. 2005), and suggest that necroptotic cell death may be a primary mode of death for a subpopulation of neurons and perhaps other cell types injured early after CCI.

Based on prior studies showing a beneficial effect of necrostatin-1 in ischemic brain injury and our previous report of reduced tissue damage in mice lacking functional TNF and Fas (Bermpohl et al. 2007), we anticipated that necrostatin-1 would reduce posttraumatic lesion size after CCI. Pretreatment with necrostatin-1 significantly reduced cavitary lesion size with a magnitude similar to that obtained in rodents using cysteine protease inhibitors or apoptosis gene knockout mice (Clark et al. 2000; Clark et al. 2006; Bermpohl et al. 2006, Bermpohl et al. 2007). Moreover, necrostatin-1 treatment conferred long lasting reduction in postinjury brain tissue damage after CCI, an effect not seen with strategies targeting caspases or Bid (Bermpohl et al. 2006; Clark et al. 2006). These data suggest that necroptotic mechanisms contribute to short- and long-term brain tissue loss after CCI.

The therapeutic window for necrostatin-1 to reduce lesion size was 15–30 minutes under the conditions of our ICV administration protocol. In contrast, ICV administration of necrostatin-1 significantly reduced ischemic infarct size even when given as late as 6 h after experimental middle cerebral artery occlusion and reperfusion (MCAO) in mice (Degterev et al. 2005). The different therapeutic window for necrostatin-1 in MCAO versus CCI may reflect different kinetics of necroptosis in the two brain injury models. In support of this possibility, we have found that the onset of loss of cellular plasmalemma integrity, a hallmark of necroptosis, peaks at 60 minutes after CCI in injured cortex and hippocampus (M Whalen, manuscript submitted). Early loss of plasmalemma integrity was also reported in another (closed head injury) TBI model (Farkas et al. 2006). In contrast, significant plasmalemma damage was not detected until 6 h after reperfusion in mice subjected to MCAO (Unal Cevik and Dalkara 2003; Unal-Cevik et al. 2004). The short therapeutic window for necrostatin-1 suggests that necroptosis is rapidly initiated after CCI, and implicate necroptotic mechanisms as one possible cause of traumatic membrane poration in the CCI model (Farkas et al. 2006; Kristensen et al. 2003; Lee et al. 1999). In support of this notion, induction of TNF and Fas receptor and assembly of TNFR1 and Fas DISC are rapid events measured in minutes to hours after experimental TBI (Beer et al. 2000; Lotocki et al. 2004; Qiu et al. 2002).

We found significant improvement in posttraumatic motor dysfunction in mice pre-treated with necrostatin-1. Necrostatin-1 also reduced sensorimotor deficits after MCAO in mice, albeit with a much longer therapeutic window compared to CCI (Degterev et al. 2005). In the current study, necrostatin-1 administration at 5 minutes after CCI was not effective in reducing postinjury motor deficits. Thus, necroptotic pathways that influence posttraumatic motor deficits may have a shorter therapeutic window for necrostatin-1 treatment compared with mechanisms responsible for cell death and cognitive outcome in the CCI model.

Perhaps the most clinically relevant finding in our study was that necrostatin-1 treatment partially reduced cognitive deficits induced by CCI. Compared to vehicle or inactive analog, necrostatin-1 led to significant improvement in injured mice in hidden platform and probe trials (the latter being a sensitive and specific test of spatial learning). The finding that necrostatin-1-treated and control groups performed equally well on visible platform trials suggests that improved MWM performance was not attributable to differences in motivation, swim speed, sensorimotor function, or other non-spatial brain functions, but likely represents improved spatial memory acquisition and retention. Necrostatin-1 improved probe trial performance in injured mice even when administered at 15 min after CCI, suggesting that necrostatin-1 might be useful for treatment of postinjury cognitive deficits in humans with TBI. Even with a narrow therapeutic window, rapid postinjury administration of necrostatins using an intravenous protocol would be feasible in patients with witnessed TBI, such as soldiers on the battlefield. Additionally, the therapeutic window for necrostatins might be longer in humans compared to mice. Studies examining the efficacy of intravenous necrostatin dosing paradigms on post-CCI cognitive deficits are currently underway in our laboratory.

Pretreatment with necrostatin-1 markedly reduced brain neutrophil influx and microglial activation at 48 h after CCI. Little is known regarding the molecular pathways that activate microglia after TBI, however a previous study showed that small molecule inhibitors of microglial activation can reduce spatial learning deficits associated with neurodegenerative disease in mice (Ralay Ranaivo et al. 2006). This report notwithstanding, reduced inflammation is not a prerequisite for improved MWM performance mediated by TNF/Fas signaling pathways (Bermpohl et al. 2007). Our data suggest that necroptotic signaling pathways contribute to cellular inflammation in injured brain, and raise the possibility that necrostatin-1 may inhibit pro-inflammatory gene expression after TBI. This hypothesis is currently under investigation in our laboratory.

The present study adds necroptosis to the list of cell death mechanisms that operate in brain after TBI. Other TBI-related cell death mechanisms include caspase-mediated apoptosis and caspase-independent programmed cell death (apoptosis inducing factor), as well as oxidative stress (Aoyama et al. 2002; Zhang et al. 2002; Zhang et al. 2005). Programmed necrosis (necroptosis) is also relevant to TBI, although further proof of this concept awaits development of specific reagents to the molecular target(s) of necrostatin-1. Further work is needed to identify necroptosis signaling pathways after TBI, and to identify the molecular target(s) that mediate protection by necrostatin-1. In addition, other necrostatins with increased activity and serum half-life should be tested in brain injury models (Jagtap et al. 2007; Wang et al. 2007).

We conclude that necroptosis, a novel form of programmed necrosis triggered by death receptors, plays a significant role in cell death and neurological dysfunction after CCI in mice. The current study provides proof of principle that necrostatin-1 and perhaps other necrostatins are promising therapeutic agents to reduce the histopathological and functional neurological sequelae of TBI.

Acknowledgments

This work was supported by grants from NIH/NINDS (RO1NS47447 to MJW) and P30NS45776.

References

Aoyama N, Katayama Y, Kawamata T, Maeda T, Mori T, Yamamoto T, Kikuchi T, Uwahodo Y. Effects of antioxidant, OPC-14117, on secondary cellular damage and behavioral deficits following cortical contusion in the rat. Brain Res 2002;934:117–124. [PubMed: 11955474]

Beer R, Franz G, Schopf M, Reindl M, Zelger B, Schmutzhard E, Poewe W, Kampfl A. Expression of Fas and Fas ligand after experimental traumatic brain injury in the rat. J Cereb Blood Flow Metab 2000;20:669–677. [PubMed: 10779011]

Bermpohl D, You Z, Korsmeyer SJ, Moskowitz MA, Whalen MJ. Traumatic brain injury in mice deficient in Bid: effects on histopathology and functional outcome. J Cereb Blood Flow Metab 2006;26:625–633. [PubMed: 16395279]

Bermpohl DYZ, Lo EH, Kim H, Moskowitz MA, Whalen MJ. TNF alpha and Fas mediate tissue damage and functional outcome after traumatic brain injury in mice. J Cereb Blood Flow Metab. 2007 In press.

Clark RS, Kochanek PM, Watkins SC, Chen M, Dixon CE, Seidberg NA, Melick J, Loeffert JE, Nathaniel PD, Jin KL, Graham SH. Caspase-3 mediated neuronal death after traumatic brain injury in rats. J Neurochem 2000;74:740–753. [PubMed: 10646526]

Clark RS, Nathaniel PD, Zhang X, Dixon CE, Alber SM, Watkins SC, Melick JA, Kochanek PM, Graham SH. boc-Aspartyl(OMe)-fluoromethylketone attenuates mitochondrial release of cytochrome c and delays brain tissue loss after traumatic brain injury in rats. J Cereb Blood Flow Metab 2007;2:316–326. [PubMed: 16736044]

Degterev A, Huang Z, Boyce M, Li Y, Jagtap P, Mizushima N, Cuny GD, Mitchison TJ, Moskowitz MA, Yuan J. Chemical inhibitor of nonapoptotic cell death with therapeutic potential for ischemic brain injury. Nat Chem Biol 2005;1:112–119. [PubMed: 16408008]

Denecker G, Vercammen D, Declercq W, Vandenabeele P. Apoptotic and necrotic cell death induced by death domain receptors. Cell Mol Life Sci 2001a;58:356–370. [PubMed: 11315185]

Denecker G, Vercammen D, Steemans M, Vanden Berghe T, Brouckaert G, Van Loo G, Zhivotovsky B, Fiers W, Grooten J, Declercq W, Vandenabeele P. Death receptor-induced apoptotic and necrotic cell death: differential role of caspases and mitochondria. Cell Death Differ 2001b;8:829–840. [PubMed: 11526436]

Farkas O, Lifshitz J, Povlishock JT. Mechanoporation induced by diffuse traumatic brain injury: an irreversible or reversible response to injury? J Neurosci 2006;26:3130–3140. [PubMed: 16554464]

Holler N, Zaru R, Micheau O, Thome M, Attinger A, Valittuti S, Bodmer JL, Schneider P, Seed B, Tschopp J. Fas triggers an alternative, caspase-8-independent cell death pathway using the kinase RIP as effector molecule. Nature Immunology 2000;1:489–495. [PubMed: 11101870]

Jagtap PG, Degterev A, Choi S, Keys H, Yuan J, Cuny GD. Structure activity relationship study of tricyclic necroptosis inhibitors. J. Med. Chem 2007;50:1886–1895. [PubMed: 17361994]

Kristensen BW, Noer H, Gramsbergen JB, Zimmer J, Noraberg J. Colchicine induces apoptosis in organotypic hippocampal slice cultures. Brain Res 2003;964:264–278. [PubMed: 12576187]

Lee RC, Hannig J, Matthews KL, Myerov A, Chen CT. Pharmaceutical therapies for sealing of permeabilized cell membranes in electrical injuries. Ann N Y Acad Sci 1999;888:266–273. [PubMed: 10842638]

Lotocki G, Alonso OF, Dietrich WD, Keane RW. Tumor necrosis factor receptor 1 and its signaling intermediates are recruited to lipid rafts in the traumatized brain. J Neurosci 2004;24:11010–11016. [PubMed: 15590916]

Matsumura H, Shimizu Y, Ohsawa Y, Kawahara A, Uchiyama Y, Nagata S. Necrotic death pathway in Fas receptor signaling. J Cell Biol 2000;151:1247–1256. [PubMed: 11121439]

Qiu J, Whalen MJ, Lowenstein P, Fiskum G, Fahy B, Darwish R, Aarabi B, Yuan J, Moskowitz MA. Upregulation of the Fas receptor death-inducing signaling complex after traumatic brain injury in mice and humans. J Neurosci 2002;22:3504–3511. [PubMed: 11978827]

Ralay Ranaivo H, Craft JM, Hu W, Guo L, Wing LK, Van Eldik LJ, Watterson DM. Glia as a therapeutic target: selective suppression of human amyloid-beta-induced upregulation of brain proinflammatory cytokine production attenuates neurodegeneration. J Neurosci 2006;26:662–670. [PubMed: 16407564]

Srinivasan A, Roth KA, Sayers RO, Shindler KS, Wong AM, Fritz LC, Tomaselli KJ. In situ immunodetection of activated caspase-3 in apoptotic neurons in the developing nervous system. Cell Death Differ 1998;5:1004–1016. [PubMed: 9894607]

Teng X, Degterev A, Jagtap P, Xing X, Choi S, Denu R, Yuan J, Cuny GD. Structure activity relationship study of novel necroptosis inhibitors. Bioorg. Med. Chem. Lett 2005;15:5039–5044. [PubMed: 16153840]

Unal Cevik I, Dalkara T. Intravenously administered propidium iodide labels necrotic cells in the intact mouse brain after injury. Cell Death Differ 2003;10:928–929. [PubMed: 12868000]

Unal-Cevik I, Kilinc M, Can A, Gursoy-Ozdemir Y, Dalkara T. Apoptotic and necrotic death mechanisms are concomitantly activated in the same cell after cerebral ischemia. Stroke 2004;35:2189–2194. [PubMed: 15256676]

Vanden Berghe T, Denecker G, Brouckaert G, Vadimovisch Krysko D, D'Herde K, Vandenabeele P. More than one way to die: methods to determine TNF-induced apoptosis and necrosis. Methods Mol Med 2004a;98:101–126. [PubMed: 15064436]

Vanden Berghe T, Kalai M, Van Loo G, Declercq W, Vandenabeele P. Disruption of HSP90 function reverts TNF-induced necrosis to apoptosis. J Biol Chem 2002;278:5622–5629. [PubMed: 12441346]

Vanden Berghe T, van Loo G, Saelens X, Van Gurp M, Brouckaert G, Kalai M, Declercq W, Vandenabeele P. Differential signaling to apoptotic and necrotic cell death by Fas-associated death domain protein FADD. J Biol Chem 2004b;279:7925–7933. [PubMed: 14668343]

Vercammen D, Beyaert R, Denecker G, Goossens V, Van Loo G, Declercq W, Grooten J, Fiers W, Vandenabeele P. Inhibition of caspases increases the sensitivity of L929 cells to necrosis mediated by tumor necrosis factor. J Exp Med 1998a;187:1477–1485. [PubMed: 9565639]

Vercammen D, Brouckaert G, Denecker G, Van de Craen M, Declercq W, Fiers W, Vandenabeele P. Dual signaling of the Fas receptor: initiation of both apoptotic and necrotic cell death pathways. J Exp Med 1998b;188:919–930. [PubMed: 9730893]

Vercammen D, Vandenabeele P, Beyaert R, Declercq W, Fiers W. Tumour necrosis factor-induced necrosis versus anti-Fas-induced apoptosis in L929 cells. Cytokine 1997;9:801–808. [PubMed: 9367540]

Wang K, Li J, Degterev A, Hsu E, Yuan J, Yuan C. Structure-activity relationship analysis of a novel necroptosis inhibitor, Necrostatin-5. Bioorg Med Chem Lett 2007;17:1455–1465. [PubMed: 17270434]

Zhang X, Chen J, Graham SH, Du L, Kochanek PM, Draviam R, Guo F, Nathaniel PD, Szabo C, Watkins SC, Clark RS. Intranuclear localization of apoptosis-inducing factor (AIF) and large scale DNA fragmentation after traumatic brain injury in rats and in neuronal cultures exposed to peroxynitrite. J Neurochem 2002;82:181–191. [PubMed: 12091479]

Zhang X, Chen Y, Jenkins LW, Kochanek PM, Clark RS. Bench-to-bedside review: Apoptosis/programmed cell death triggered by traumatic brain injury. Crit Care 2005;9:66–75. [PubMed: 15693986]

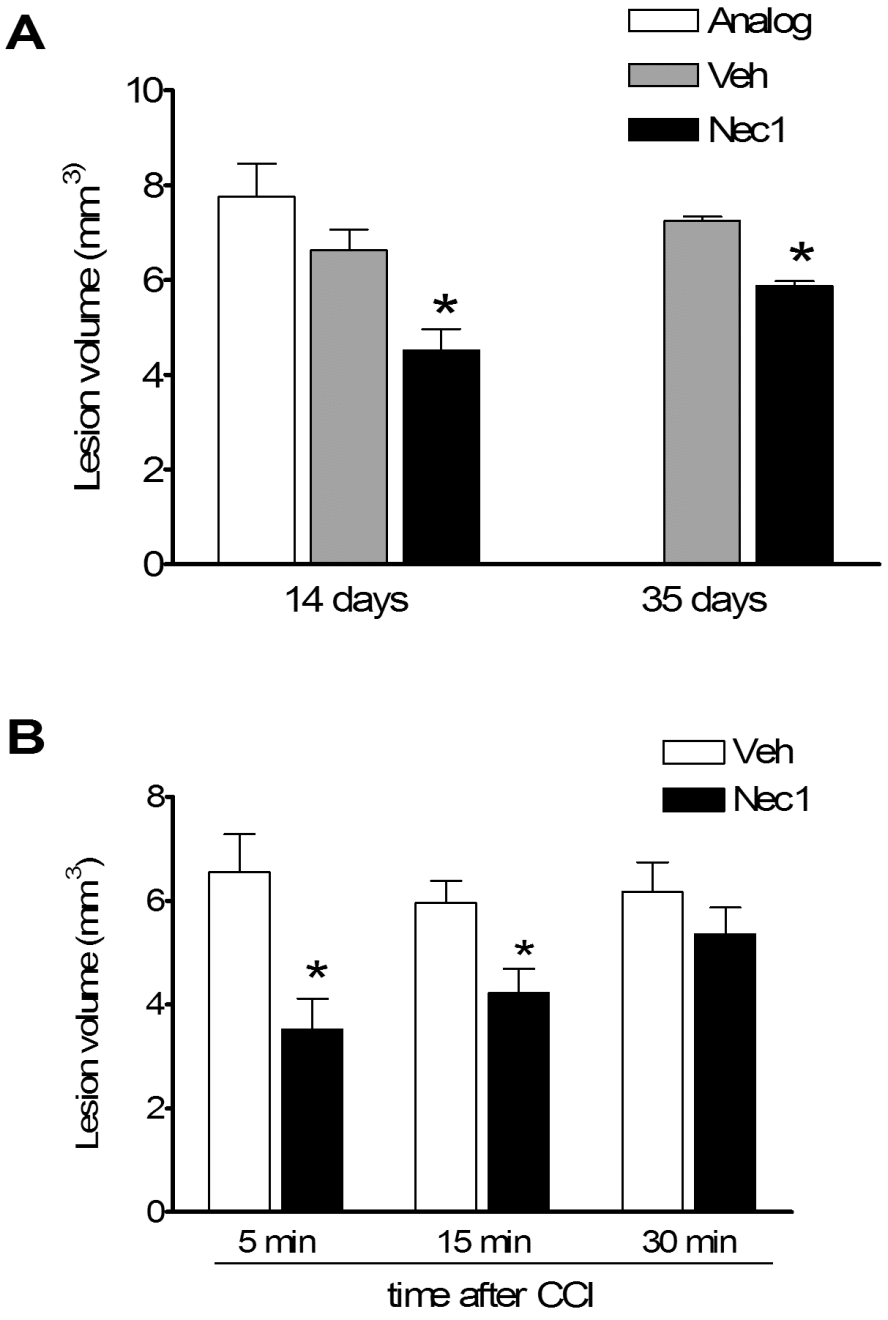

Figure 1.

Brain lesion volume is reduced in Necrostatin-1 treated mice after controlled cortical impact (CCI). (A) Pretreatment with necrostatin-1 reduced lesion volume at 14 days after CCI compared to treatment with vehicle (Veh) or inactive analogue (ANA)($p < 0.001$ ANOVA, *$p < 0.05$ versus ANA or Veh). Pretreatment with necrostatin-1 also reduced lesion size assessed at 35 days (*$p < 0.05$). For 14 days, n = 7–16/group; for 35 days, n = 4/group). (B) Necrostatin-1 was administered after CCI at the times indicated. Post injury treatment with necrostatin-1 reduced lesion size compared to vehicle when administered at 5 or 15 min but not 30 min after CCI (*$p < 0.05$, n = 4–5/group).

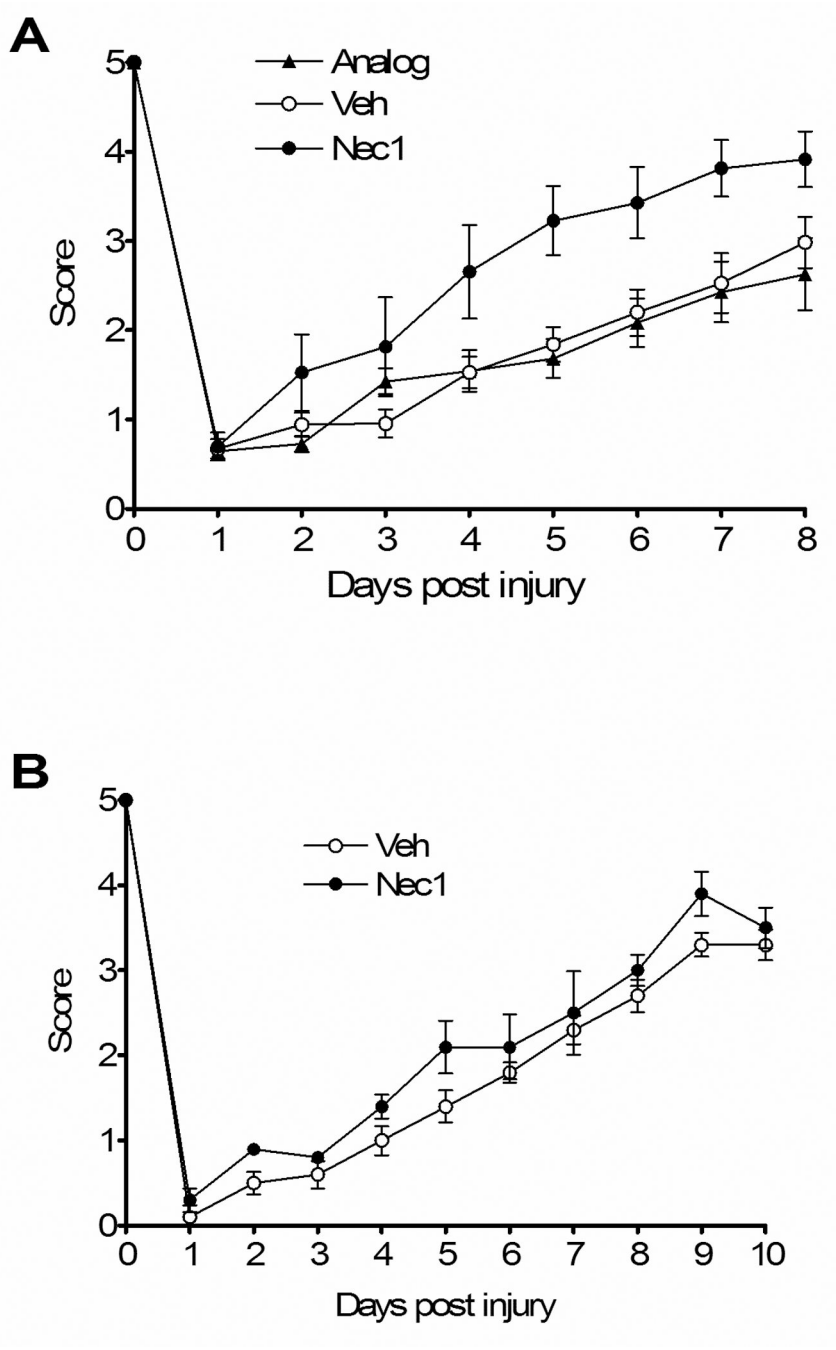

Figure 2.

Reduced motor deficits after controlled cortical impact (CCI) in Necrostatin-1 treated mice. Vestibulo-motor function assessed by the wire grip test was similar among all groups prior to CCI. Post injury motor function was significantly improved in mice administered necrostatin-1 (Nec-1) compared to inactive analogue (ANA) or vehicle (Veh) ($p < 0.05$ for group effect, n=8/group). (B) Administration of necrostatin-1 (n = 5) to mice 5 min after CCI did not affect motor performance vs. vehicle treated animals (n = 9).

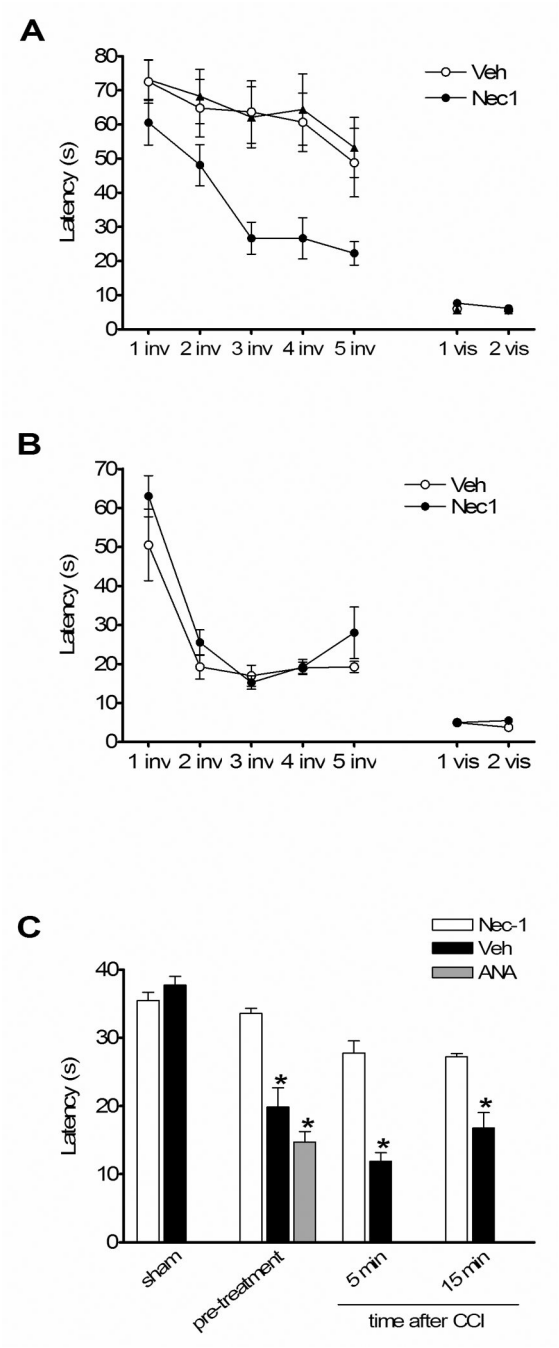

Figure 3.

Necrostatin-1 treatment improves Morris water maze (MWM) performance after controlled cortical impact (CCI). (A) Morris water maze performance in naive adult animals administered necrostatin-1 (Nec-1) or vehicle (Veh). No difference in performance was observed between uninjured Veh- and Nec-1-treated mice in hidden or visible platform trials, or in probe trials (n=4/group). (B) Performance in the hidden platform trials was significantly improved in animals pretreated with Necrostatin-1 versus inactive analogue (ANA) or vehicle (Veh) ($p < 0.05$ for group effect, n = 7/group). (C) Probe trial performance in mice administered Necrostatin-1 (Nec-1) vs. Veh or ANA. No effect of drug treatment was observed in sham injured mice on probe trial performance, however injured mice administered Nec-1 before or

at 5 or 15 minutes after CCI had improved performance vs. vehicle-treated animals (*$p < 0.05$), n= 4–9/group).

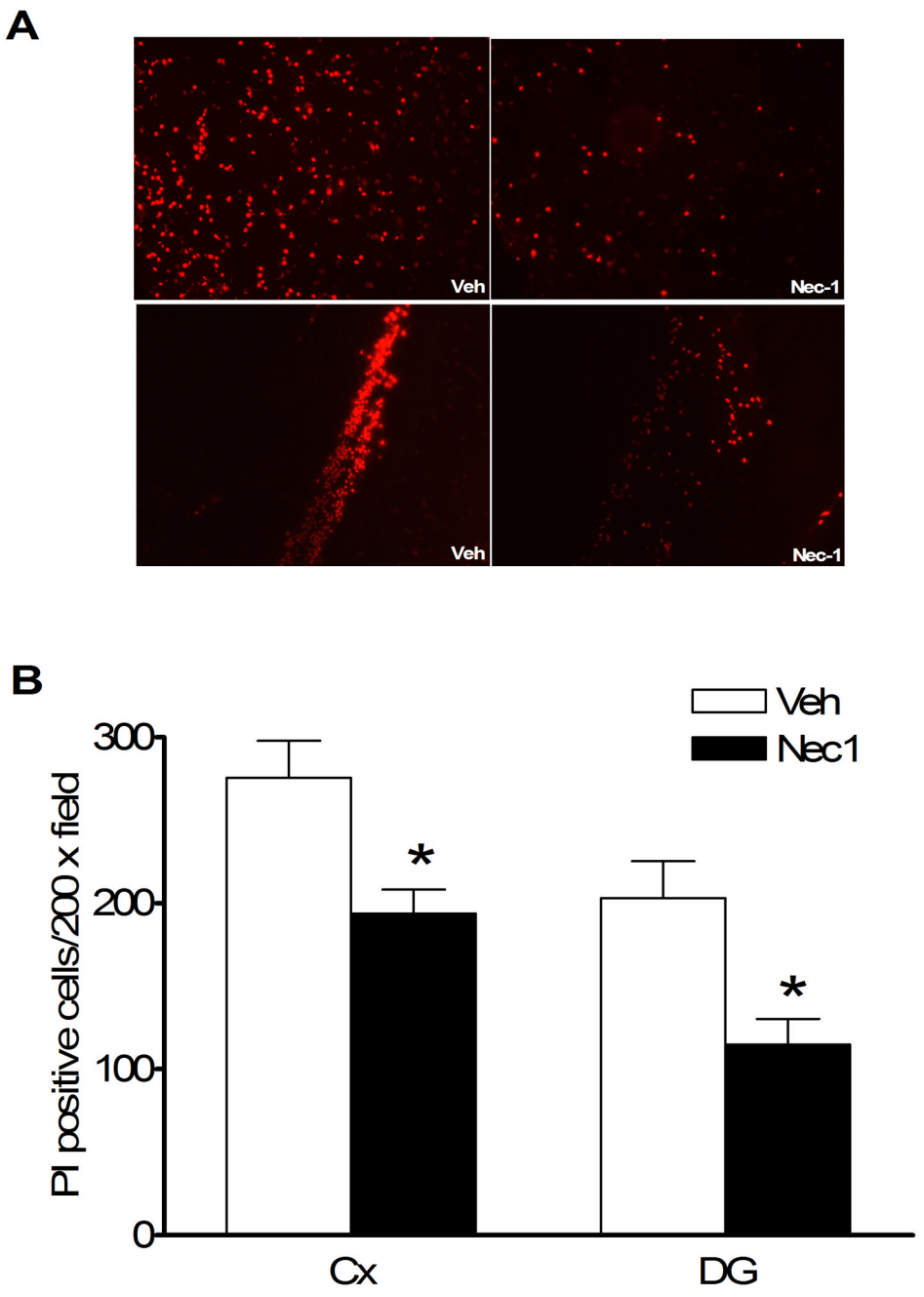

Figure 4.

Pre-treatment with necrostatin-1 (Nec-1) reduces propidium iodide (PI)-positive cells at 6 h after controlled cortical impact (CCI) in injured cortex and hippocampus. (A) Representative photomicrographs showing reduced numbers of PI-positive cells in cortical and dentate gyrus brain regions after CCI in Nec-1 and vehicle-treated mice. Magnification × 200. (B) Quantitation of PI-positive cells in injured cortex and dentate gyrus. *$p < 0.01$ vs. vehicle treated animals (n = 12/group).

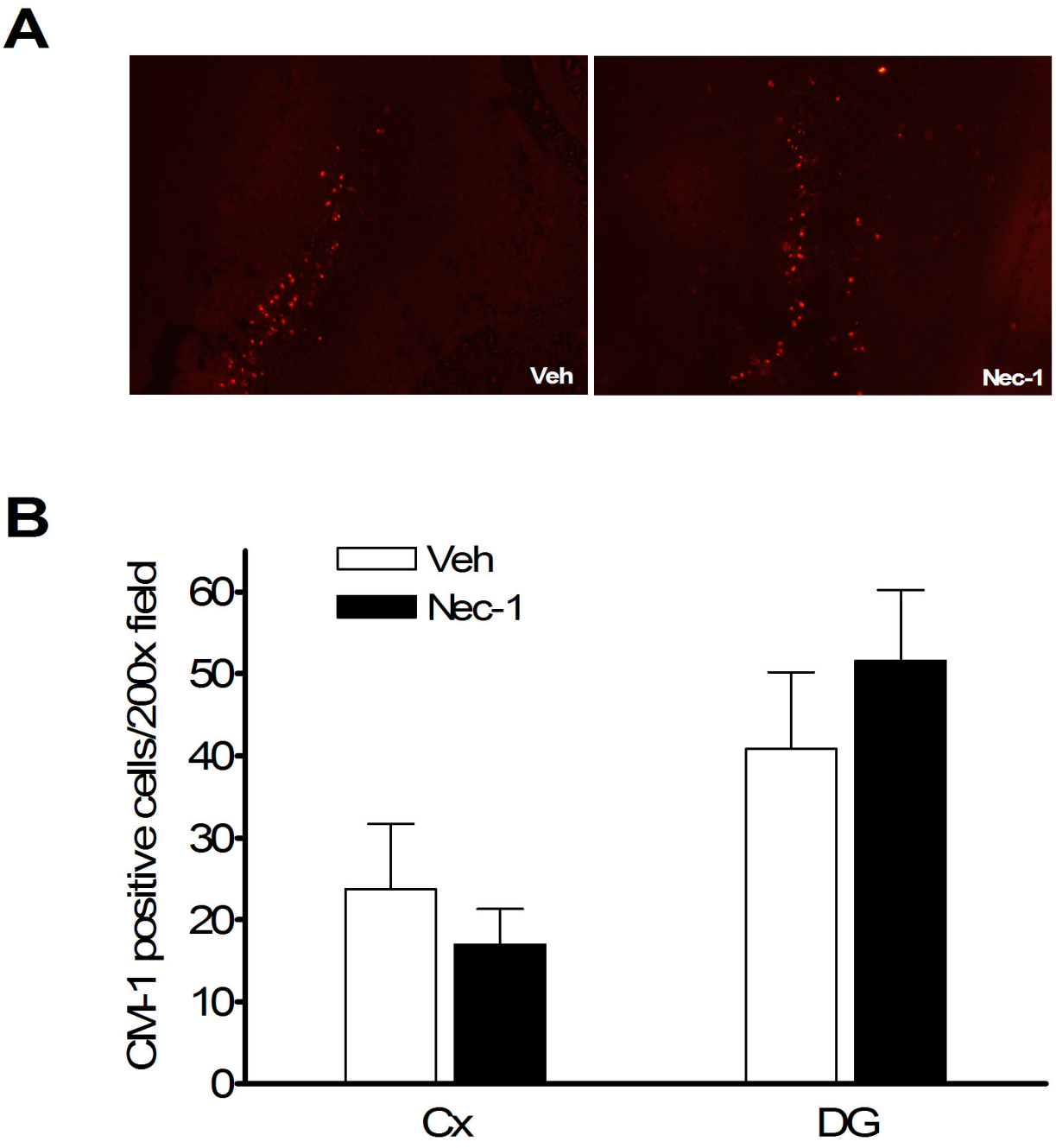

Figure 5.
No effect of necrostatin-1 on caspase-3-positive cells after controlled cortical impact. Necrostatin-1 or vehicle was administered to mice (n = 7–9/group) immediately before CCI and caspase-3 positive cells were quantitated in injured cortex and dentate gyrus at 48 h. (A) Representative photomicrographs showing similar numbers of caspase-3-positive cells in dentate gyrus after CCI in Necrostatin-1 (Nec-1) and vehicle-treated (Veh) mice. (B) Quantitation of caspase-3-positive cells in injured cortex and dentate gyrus.

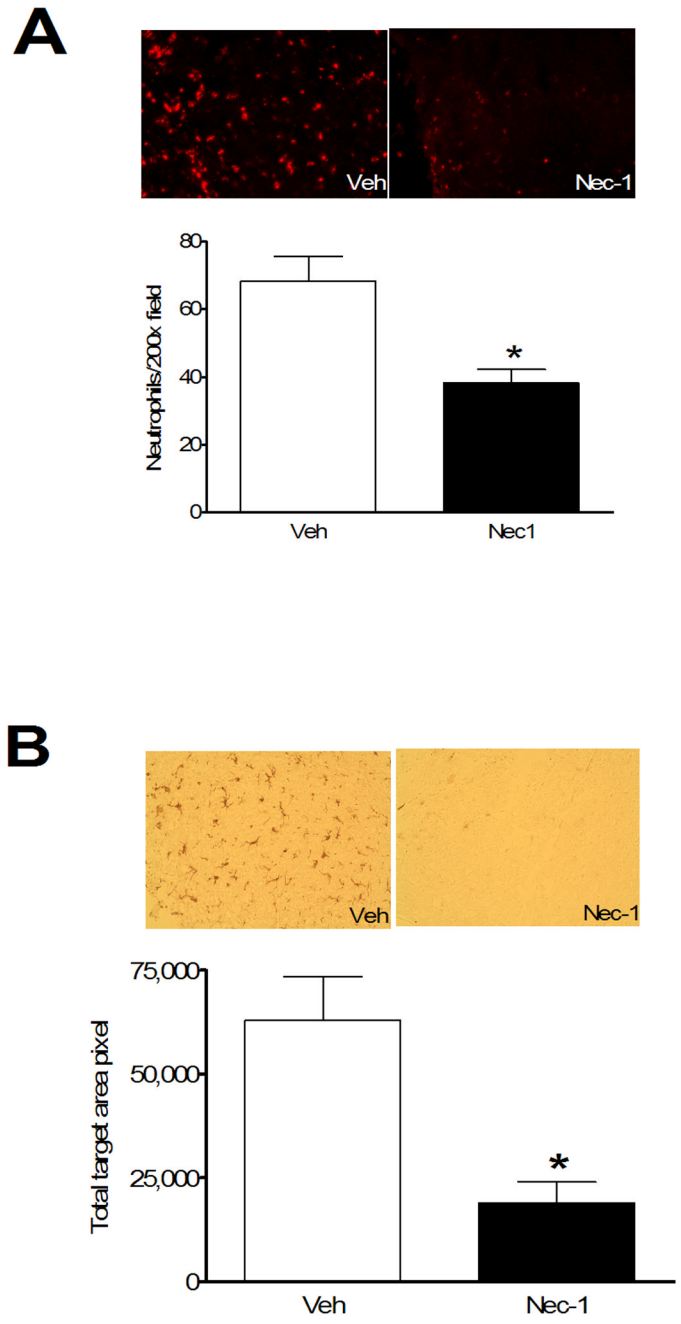

Figure 6.

Pre-treatment with necrostatin-1 reduces neuroinflammation assessed at 48 h after controlled cortical impact. (A) Representative photomicrographs (top panels) showing neutrophil accumulation in injured cortex in mice administered vehicle (Veh) or necrostatin-1 (Nec-1). Bottom panels show quantitation of neutrophils in injured cortices of Veh and Nec-1 treated mice. * $p < 0.05$ vs. Veh (n = 10–11/group). (B) Marked reduction in microglial activation in mice administered necrostatin-1 vs. vehicle prior to controlled cortical impact. Upper panels show representative immunohistochemical staining using the microglial specific marker IBA-1. The graph in the lower panel shows quantitation of microglial activation using image

analysis software. *$p < 0.05$ vs. vehicle ($n = 7–9$/group). Magnification × 200 in all photomicrographs.